Received: 21 November 2019 | Revised: 14 April 2020 | Accepted: 18 April 2020

DOI: 10.1002/rth2.12366

ORIGINAL ARTICLE

rpth research & practice in thrombosis & haemostasis

Rate zonal centrifugation can partially separate platelets from platelet-derived vesicles

Linda G. Rikkert MSc[1,2,3] | Mendel Engelaer BSc[2,3] | Chi M. Hau[2,3] | Leon W. M. M. Terstappen MD, PhD[1] | Rienk Nieuwland PhD[2,3] | Frank A.W. Coumans PhD[2,3]

[1]Department of Medical Cell BioPhysics, University of Twente, Enschede, The Netherlands

[2]Amsterdam UMC, Laboratory of Experimental Clinical Chemistry, University of Amsterdam, Amsterdam, The Netherlands

[3]Amsterdam UMC, University of Amsterdam, Vesicle Observation Center, Amsterdam, The Netherlands

Correspondence
Linda G. Rikkert, Amsterdam UMC, University of Amsterdam, Laboratory of Experimental Clinical Chemistry, Meibergdreef 9, 1105 AZ Amsterdam, the Netherlands.
Email: l.g.rikkert@amsterdamumc.nl

Funding information
This work was supported by the Netherlands Organisation for Scientific Research – Domain Applied and Engineering Sciences (NWO-TTW), research programs VENI 13681 (FC), and Perspectief CANCER-ID 14198 (LR).

Handling Editor: Prof. Yotis Senis

Abstract

Background: Centrifugation is commonly used as a first step to enrich biomarkers from blood. Biomarkers are separated on the basis of density and/or diameter. However, the centrifugation protocol affects the yield and purity of biomarkers, for example, isolation of platelets results in co-isolation with extracellular vesicles (EVs).

Objective: To assess the ability of rate zonal centrifugation (RZC) to separate platelets from co-isolated EVs.

Methods: Using a linear Optiprep gradient, RZC was able to separate a mixture of beads with different diameters but similar density. Next, RZC was applied to samples containing both platelets and platelet-derived EVs (n = 3). After RZC, all fractions were collected and stained with anti-CD61-Alexa 488 to measure the concentrations of platelets and platelet-derived EVs by flow cytometry.

Results: We confirm that RZC separates polystyrene beads with diameters of 140 nm, 380 nm and 1,000 nm. Next, we show that the majority of platelets occur in fractions 8-19, whereas the majority of platelet-derived EVs are detectable in fractions 1-7. Furthermore, each fraction contains a different diameter range of platelets, which suggests that separation is indeed diameter based.

Conclusion: RZC can partially separate platelets from EVs.

KEYWORDS

biomarkers, blood platelets, centrifugation, extracellular vesicles, flow cytometry

Essentials

- Centrifugation of whole blood results in co-isolation of platelets and extracellular vesicles (EVs).
- Rate zonal centrifugation (RZC) is tested to separate platelets from EVs.
- Fractions collected after RZC are compared for concentrations of platelets and EVs.
- RZC can partially separate platelets from EVs.

1 | INTRODUCTION

The isolation of a biomarker from a body fluid is essential to evaluate the importance of the biomarker. Centrifugation is frequently applied to isolate biomarkers from whole blood on the basis of differences in density and/or diameter.[1-5] The distance a particle travels through a solution during centrifugation can be approximated using the Stokes equation:

$$\Delta x = \frac{d^2(\rho_P - \rho_M)gt}{18n} \quad (1)$$

and depends on the diameter (d) and volumetric mass density (ρ_P) of the particle relative to the volumetric mass density (ρ_M) and viscosity (η) of the gradient. The g refers to the gravitational acceleration and the t to the time. Using this equation, we demonstrated that centrifugation protocols used to isolate biomarkers from blood from cancer patients result in impure biomarkers, due to the co-isolation and thus contamination with other biomarkers; for example, the isolation of tumor-educated platelets results in co-isolation with tumor-derived extracellular vesicles (EVs) and vice versa.[6,7]

A commonly applied centrifugation method is density gradient centrifugation, where a sample is loaded on top of a density gradient. During density gradient centrifugation, particles move down the gradient until the difference between particle density and medium density is zero. Therefore, the separation principle is based on the density of a particle. In contrast, with rate zonal centrifugation (RZC), the gradient has a lower density throughout the entire gradient compared to density gradient centrifugation to ensure that the distance a particle travels through the gradient is solely depends on the particle diameter (Equation 1). RZC has previously been applied to isolate viruses, DNA, lysosomes, and other nanoparticles.[8-10]

At present, there is great interest to enhance the purity of biomarkers to improve the interpretation of data. In this study, we applied an earlier described protocol to isolate a cancer biomarker from human blood, that is, "tumor-educated platelets," and demonstrate that this protocol produces a mixture of 2 biomarkers, platelets and EVs, which we partially separate by RZC.

2 | MATERIALS AND METHODS

RZC requires loading of a sample on top of a gradient. If a single-step gradient is used, the transition between sample and gradient can cause particles in the sample to form clusters at the top of the gradient. These clusters are bigger in diameter and have a higher sedimentation speed compared to single particles (Equation 1). These clusters end up in the pellet or mix with the surrounding media and spread throughout the tube. This process is called droplet sedimentation.[11] Based on preliminary results, we know that using a linear gradient in which the density increases toward the bottom of the tube prevents droplet sedimentation. Furthermore, the linear gradient has a slightly higher viscosity than the sample to facilitate sample loading without mixing with the gradient.

2.1 | Linear density gradient

A gradient mixer (supplier unknown) was applied to generate a linear density gradient of 4% at the top to 8% Optiprep at the bottom (60% [w/v] solution of iodixanol in water; Sigma-Aldrich, St Louis, MO, USA), see Figure 1. Bagamery et al[12,13] describe that sample manipulation-related platelet activation can be minimized by using Optiprep. Optiprep was diluted in 0.22-µm filtered (Merck Millipore, Burlington, MA, USA) phosphate-buffered saline (PBS; 154 mM NaCl, 1.24 mM $Na_2HPO_4.2H_2O$, 0.2 mM $NaH_2PO_4.2H_2O$, pH 7.4). The gradient mixer chambers were filled with 4% Optiprep (ρ = 1.027 g/mL) and 8% Optiprep (ρ = 1.048 g/mL), respectively. Depletion of medium from the high-density chamber causes medium from the low-density chamber to flow into the high-density chamber, where a magnetic stirrer mixes the media. A peristaltic pump (Minipuls 3; Gilson, Lewis Center, OH, USA) pumped medium into a stainless steel syringe needle (alloy 316, 18 gauge, 6 inch pipetting blunt 90°

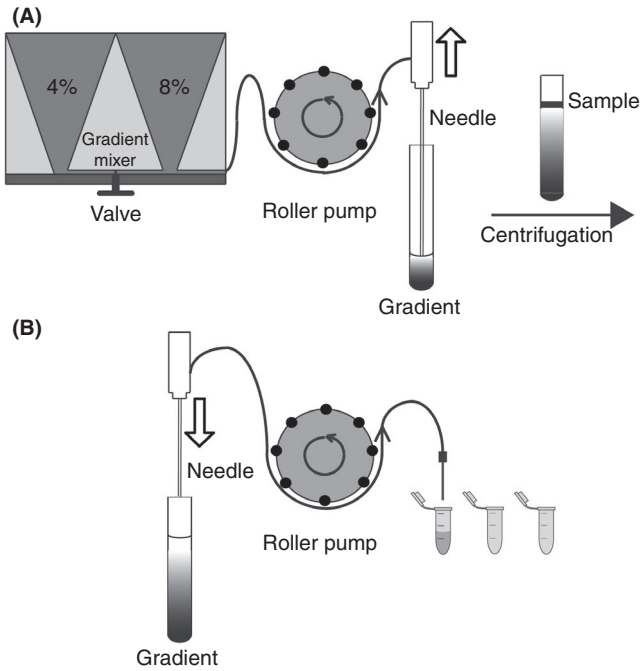

FIGURE 1 Gradient setup. A, A 4% Optiprep solution is loaded into the left compartment of the gradient mixer. The 8% Optiprep solution is loaded into the right compartment of the gradient mixer together with a magnetic stirring bar. The 4% Optiprep is pumped into the gradient mixer using a roller pump, mixed with the 8% Optiprep by stirring, and layered into a centrifuge tube using a needle mounted to an injection pump. The Optiprep concentration gradually decreases to form a linear gradient. B, After sample loading and centrifugation the gradient is placed back into the setup. A needle is mounted to an injection pump. The needle is lowered while extracting the fractions into Eppendorf tubes using a roller pump

tip; Sigma-Aldrich). The needle tip was held at the meniscus by an injection pump (Perfusor secura FT; B. Braun Medical, Bethlehem, PA, USA). In this fashion, a continuous linear Optiprep gradient was generated in the gradient tube (10 mL; Sarstedt, Newton, NC, USA). The optical density of successive fractions collected from 3 gradients was measured using a microplate reader (340 nm line, Spectramax i3; Molecular Devices, San Jose, CA, USA) to demonstrate the linearity of the gradient (Figure S1A). Gradients were stored at 4°C and used within 2 days after equilibration to room temperature.

2.2 | Bead mixture

One hundred forty– and 380-nm green fluorescent polystyrene beads and 1,000-nm nonfluorescent beads (Thermo Fisher Scientific, Waltham, MA, USA) were used to validate the RZC setup. Each bead concentration was 0.03% w/v in 0.22-µm filtered PBS supplemented with 0.1% sodium dodecyl sulfate in distilled water (20% SDS stock; Bio-Rad Laboratories Inc, Hercules, CA, USA).

2.3 | Platelets and platelet-derivedEVs

Blood was obtained from 3 healthy donors with informed consent in accordance with the Helsinki Declaration and approved by the medical-ethical assessment committee of the Academic Medical Center, University of Amsterdam. Blood collection and handling were according to the earlier described protocol of Best et al[1] to reproduce the isolation of "tumor-educated platelets." For each donor, whole blood was drawn using a 21G needle, and the first vacutainer was discarded. Next, two 4.0 mL ethylenediaminetetraacetic acid (EDTA) vacutainers (BD Biosciences, Franklin Lakes, NJ, USA) were collected, mixed by gentle inversion and processed within 15 minutes. To obtain "tumor-educated platelets," vacutainers were centrifuged at 120 *g* for 20 minutes at 20°C and without brake in a Rotina 380R centrifuge (Hettich, Tuttlingen, Germany) to prepare platelet-rich plasma. The platelet-rich plasma was transferred to a 10-mL conical base tube (Sarstedt), and centrifuged at 360 *g* for 20 minutes at 20°C and without brake to concentrate the platelets. The platelets were washed twice with 1 mL of 0.05-µm filtered (Nuclepore; GE Healthcare, Chicago, IL, USA) 0.8% EDTA buffer (Titriplex III in PBS; Merck Millipore, Billerica, MA, USA). Finally, 500 µL of 0.8% EDTA buffer was added to the pellet, and the pellets were pooled. After each centrifugation step, supernatant above the pellet was removed, leaving some supernatant so the pellet was not disturbed. Therefore, plasma was still present when the washed pellets were pooled.

The mixture of platelets and EVs (1 mL) was loaded on size exclusion chromatography (SEC) columns (10-mL qEVoriginal; Izon Science, Christchurch, New Zealand) to replace the blood plasma with 0.05 µm of filtered acid citrate dextrose buffer (5 parts PBS to 1 part acid citrate dextrose; 0.85 mol/L trisodium citrate, 0.11 mol/L D-glucose and 0.071 mol/L citric acid, supplemented with 0.32% trisodium citrate in PBS, pH 7.4; see Figure S2). Fractions 8 and 9 contained all particles >70 nm, both platelets and EVs. These fractions were pooled for each donor as starting material for RZC.

2.4 | Centrifugation and fractionation

Five hundred microliters of starting material was loaded on the 4%-8% Optiprep gradient using a plastic Pasteur pipette (VWR, Radnor, PA, USA), which was placed against the wall of the tube just above the gradient. For the bead mixture, RZC was performed at 2772 *g* for 100 minutes at 20°C and without brake. Using Equation 1, we predicted which combination of centrifugal force and time was needed to make sure the platelets would end up in the last fractions and EVs could spread out in the first fractions. RZC of the platelet- and EV-containing samples was performed at 1000 *g* for 30 minutes at 20°C and with acceleration and deceleration set to the minimum possible value. Centrifugation was performed at 20°C, since platelets are more sensitive to activation at 4°C.[14]

Figure 1B shows the fractionation setup. A needle aspirating from the top was used for fractionation.[15] The tip of the needle was held at the meniscus while extracting twenty 0.5 mL fractions into Eppendorf tubes (Greiner Bio-One, Kremsmünster, Austria) using a peristaltic pump. Each fraction was weighed on an analytical balance (Sartorius, Göttingen, Germany) to determine the collected volume per fraction. Figure S1B shows that 87.7% (50/57) of the collected fractions were within the mean collected volume ±40 µL (~1 droplet). The volume per fraction was used to calculate the platelet and platelet-derived EV yield, which was defined by the percentage of platelets found in all fractions compared to the starting material. The platelet yield ranged from 30% to 40%, whereas the platelet-derived EV yield ranged between 66% and 146%.

2.5 | Flow cytometry

Flow cytometry measurements were performed on an A60-Micro (Apogee, Middlesex, UK) at a flow rate of 3.0 µL/min. Samples were measured triggered on 405-nm side scatter. The side scatter trigger threshold corresponds to a side scattering cross section of 10 nm^2 (Rosetta Calibration; Exometry, Amsterdam, The Netherlands).

Bead samples were prediluted in 0.22 µm of filtered PBS if necessary to event rates below 5,000/s to prevent swarm when triggering on side scatter.[16] Bead samples were measured for 1 minute. Side scatter resulted in distinct bead populations.

To obtain the platelet and platelet-derived EV concentration by flow cytometry, 20 µL of each fraction was incubated with 2.5 µL anti-CD61-Alexa 488 (Y2/51, final concentration 0.01 mg/mL; Bio-Rad Laboratories) aggregates in the antibody solution removed by centrifugation at 18 890 *g* for 5 minutes at 20°C for 2 hours at room temperature in the dark. The labeling was stopped by adding 200 µL of PBS (21-031-CV; Corning, Corning, NY, USA) to the samples. The experiment with the platelet- and EV-containing samples was performed at a later date than the bead sample. In the meantime, we

switched from custom-made PBS to commercially available PBS. Samples were measured for 2 minutes triggered on 405-nm side scatter. We selected 1 minute of data in which the flow rate was stable. A distinct platelet population was identified by side scatter and Alexa 488 fluorescence, and platelet-derived EVs were identified by a gate at the Alexa 488 fluorescence channel exceeding background fluorescence levels in the unstained sample (sample without antibody), corresponding to 397 molecules of equivalent soluble fluorochrome fluorescein isothiocyanate (see Figure 3).

Provided concentrations are the number of detected particles multiplied by total sample dilution divided by flow rate and measurement time. Data were analyzed using FlowJo (v10.4.2; FlowJo LLC, Ashland, OR, USA), and statistical analysis was performed in Prism 7.0 (GraphPad Software, La Jolla, CA, USA). We used Rosetta Calibration v1.08 (Exometry) to calibrate side-scattered light to units of newtons per square meter and to relate side-scattered light to the diameter (>200 nm) of platelets and platelet-derived EVs.[17] We modeled platelets as solid spheres with a refractive index (RI) of 1.40 [18] using steps of 10 nm in diameter.

3 | RESULTS

3.1 | RZC of beads

We applied a mixture of beads of various diameters to validate that RZC separates particles with the same density but a different diameter. After centrifugation, distinct bands are observed in the gradient (Figure 2). The position of the 140-nm and 380-nm beads are indicated and arrows indicate the *expected* positions of the 140-nm and 380-nm beads after RZC based on Equation 1. The 2 extra bands seen below the 380-nm beads are likely doublets and triplets of the 380-nm beads. The graph shows the percentage of beads from the whole bead population measured by flow cytometry, with the peak percentage of beads in the same fraction as the bands. The flow cytometry data show substantial broadening of the peaks, which is likely caused by the fraction collection method we used because the fraction boundaries can coincide with the bead bands.

3.2 | RZC of platelets and platelet-derived extracellular vesicles

The starting material contained both platelets and platelet-derived EVs and was loaded on top of the gradient before centrifugation; see Figure 3 and S3. Almost no platelets are observed in fractions 1-5, and the majority of platelets are observed in fractions 8-19, with an average scatter signal on the *y*-axis increasing when moving further down the gradient (Figures 3 and 4A and Figure S3). Figure 4B shows that the mean diameter of platelets increases while moving down the gradient, confirming that each fraction contains platelets with a different diameter range.

The majority of platelet-derived EVs (64, 84, and 77% for donors 1, 2, and 3, respectively) is observed in fractions 1-7 (Figures 3 and 4A; a logarithmic scale was used for the *y*-axis of Figure 4A as the platelet-derived EV concentrations of donors 2 and 3 are low compared to donor 1).

4 | DISCUSSION

The use of biomarkers is complicated by their differences in physical characteristics such as density and diameter. Moreover, during

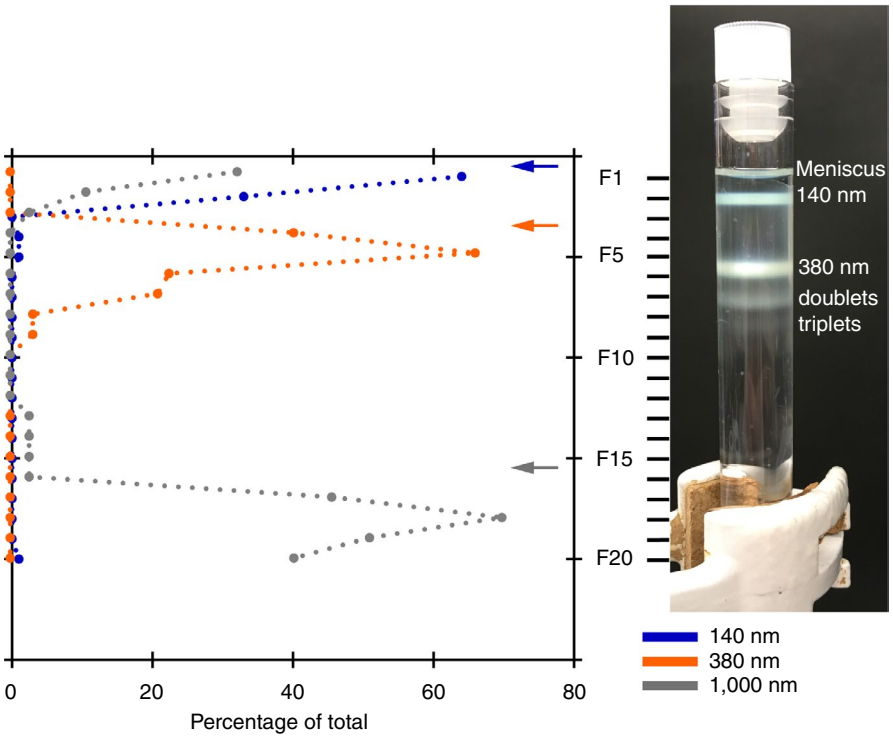

FIGURE 2 Rate zonal centrifugation of a bead mixture. A mixture of polystyrene beads with the same density but different diameter (140 nm, 380 nm and 1,000 nm) is loaded on top of a 4%-8% Optiprep gradient. After centrifugation at 2,772 *g* for 100 minutes, the bead populations are visible as distinct bands. This is confirmed by the peaks in the flow cytometry data, which also reveal the 1,000-nm beads, which are not visible by eye because they are not fluorescent. The arrows show the expected position of each bead population calculated based on the Stokes equation

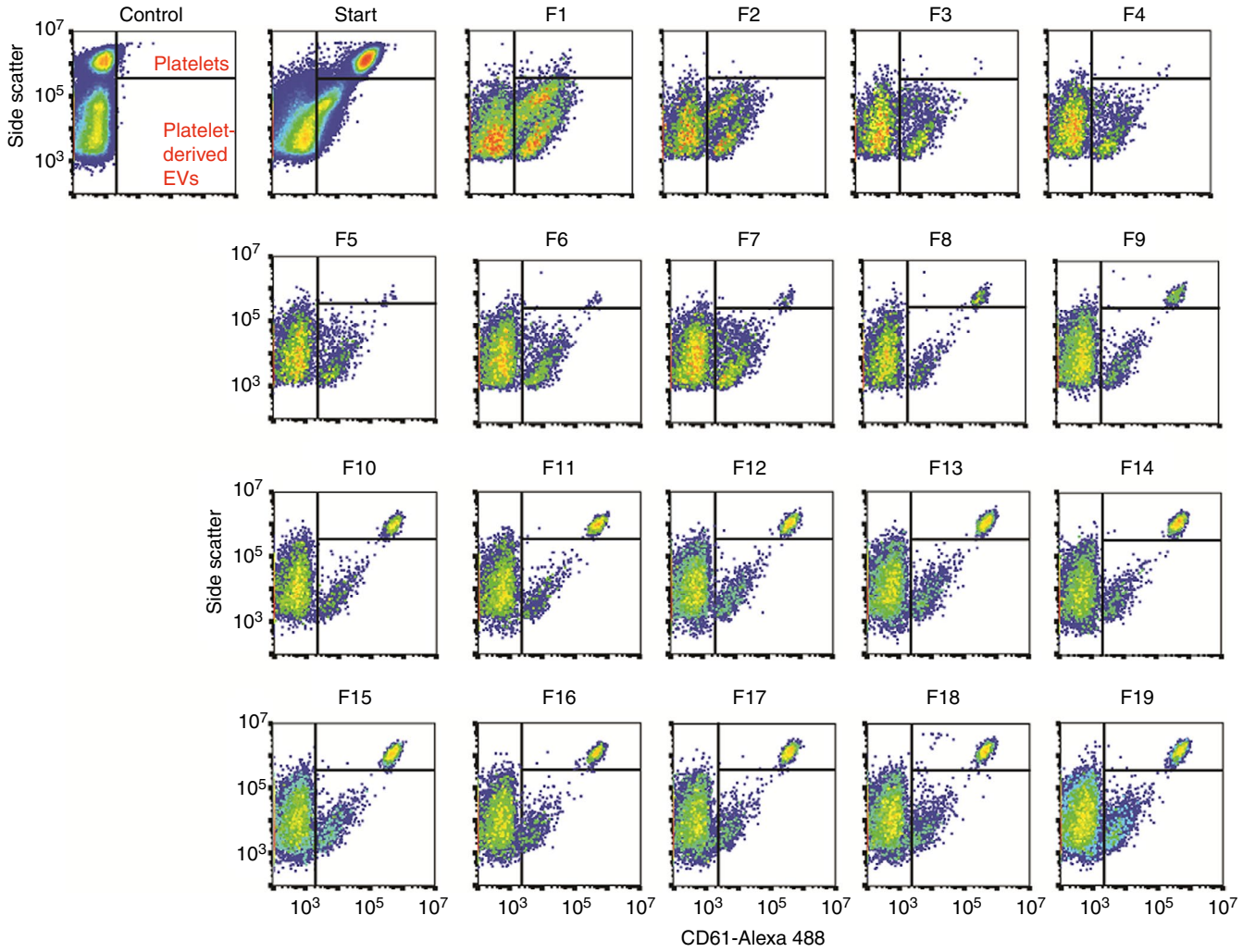

FIGURE 3 Flow cytometry scatter plots of platelets and platelet-derived extracellular vesicles (EVs) in fractions of rate zonal centrifugation (RZC) from a representative donor. The first graph shows the gates set for platelets and platelet-derived EVs for the unstained starting material (control). The starting material, loaded on top of the gradient before centrifugation, contained both platelets and platelet-derived EVs. The platelet population is missing in the first fractions. However, moving further down the gradient shows that the platelets are mainly present in fractions 8-19 and the scatter signal on the *y*-axis shifts while moving down through the gradient. The majority of platelet-derived EVs is present in fractions 1-7. In fractions 1 and 2, we observed 2 subpopulations of CD61 + EVs, of which the upper population is not observed in the other fractions. At present, we have no explanation for the presence of this subpopulation

sample preparation biomarkers are frequently co-isolated. To overcome these limitations, we introduce RZC as a technique to separate biomarkers. RZC is not an alternative method to isolate platelets and EVs from blood. The goal of this article was to show as a "proof of principle" that particles with a likely similar density can be separated by RZC on the basis of size.

RZC has never been applied to samples containing mixtures of platelets and EVs. We demonstrate that platelets and platelet-derived EVs can indeed be partially separated by RZC. Furthermore, the platelet diameter range differs slightly in each fraction, suggesting that RZC may be used to isolate monodisperse platelet or EV populations. Calibration of detection instruments is currently performed using polystyrene and silica beads. However, these beads differ in RI compared to EVs.[19] Therefore, monodisperse biological reference material of, for example, EVs is preferred to calibrate detection techniques because then corrections for differences in RI are not necessary.

Lipoproteins present in the starting material can independently migrate through the gradient, although the density for lipoproteins is too low and the diameter is too small to travel through the gradient in the configuration as used in the present study.[20] Comigration of lipoproteins with platelets and/or EVs is possible, and this would affect the density and size of platelets and/or EVs and therefore the fraction in which a platelet or an EV accumulates. Nevertheless, these effects are mitigated by removal of the majority of lipoproteins by SEC prior to RZC.[21]

Figure 2 shows a difference between the expected and measured results. The linear increasing density and viscosity throughout the gradient make it difficult to predict the precise location of the beads by using Equation 1. Therefore, we also tested in practice before adjustments were definitive. RZC relies on the assumption that the density between particles in a solution is equal. In this study, we assumed that the densities of platelets and EVs are equal. However,

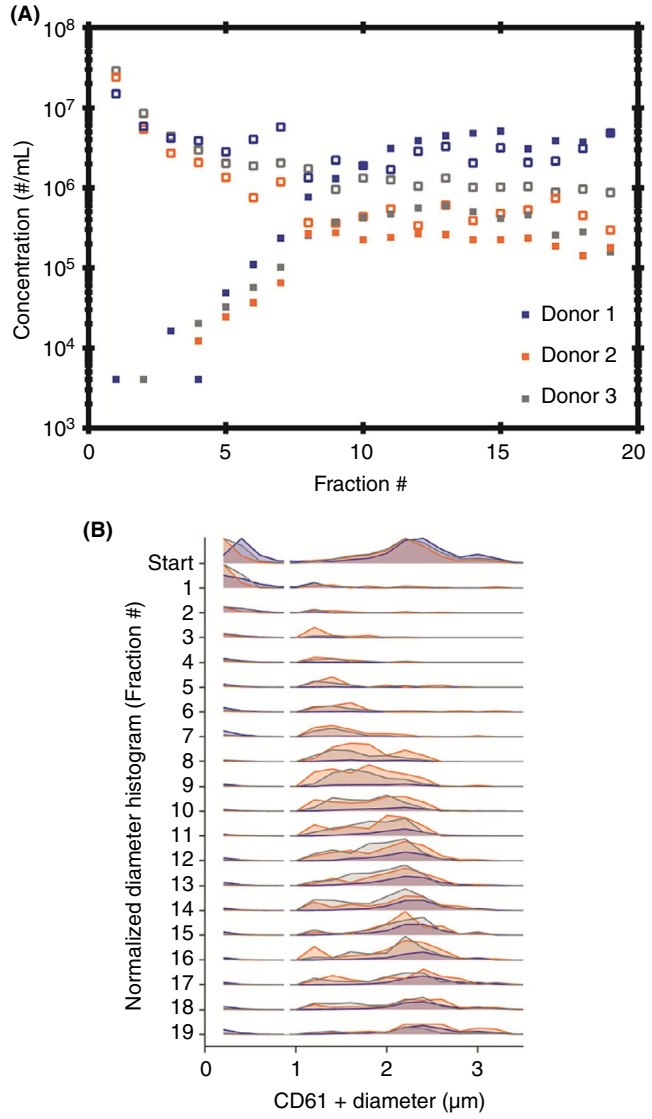

FIGURE 4 Platelet and platelet-derived extracellular vesicles (EV) concentration and diameter measured in rate zonal centrifugation fractions (RZC) for 3 donors. A, The highest concentration of platelets (closed symbols) are present in fractions 8-17. The highest concentration of platelet-derived EVs (open symbols) are present in fractions 1-7. B, The platelet and platelet-derived EV diameter in RZC fractions for donors 1-3. The platelet diameter range (>1 µm) was obtained using Rosetta calibration. The platelet diameter range shifts to the right while moving through the gradient, which confirms that the separation of platelets from platelet-derived EVs (200 nm to 1 µm) by RZC is based on diameter

the density of platelets is reported to range between 1.061 and 1.091 g/mL[22,23] and the density of EVs between 1.02 and 1.19 g/mL.[24-27] Therefore, an overlap in platelet diameter range is shown in the different fractions. Furthermore, we have to keep in mind that activated platelets may change in shape, density, and diameter.[28]

In conclusion, based on the results from the bead mixture, we show that RZC can be used to separate particles with the same density but a different diameter. Furthermore, we applied RZC to a biological sample and show that RZC can partially separate platelets from EVs.

RELATIONSHIP DISCLOSURE

The authors declare nothing to report.

AUTHOR CONTRIBUTIONS

LR, ME, RN, LT, and FC contributed to the concept and design of the study. LR, ME, and CH acquired the data. LR and ME analyzed the data. LR, ME, RN, LT, and FC interpreted the data. LR wrote the manuscript. ME, RN, LT, and FC reviewed and made critical revisions to the manuscript and approved the final version to be published.

REFERENCES

1. Best MG, Sol N, Kooi I, Tannous J, Westerman BA, Rustenburg F, et al. RNA-Seq of tumor-educated platelets enables blood-based pan-cancer, multiclass, and molecular pathway cancer diagnostics. Cancer Cell. 2015;28(5):666–76.
2. van Eijndhoven MA, Zijlstra JM, Groenewegen NJ, Drees EE, van Niele S, Baglio SR, et al. Plasma vesicle miRNAs for therapy response monitoring in Hodgkin lymphoma patients. JCI Insight. 2016;1(19):e89631.
3. Coumans FAW, Doggen CJM, Attard G, de Bono JS, Terstappen LWMM. All circulating EpCAM+CK+CD45- objects predict overall survival in castration-resistant prostate cancer. Ann Oncol. 2010;21(9):1851–7.
4. Dawson S-J, Tsui DW, Murtaza M, Biggs H, Rueda OM, Chin S-F, et al. Analysis of circulating tumor DNA to monitor metastatic breast cancer. N Engl J Med. 2013;368(13):1199–209.
5. Heidary M, Auer M, Ulz P, Heitzer E, Petru E, Gasch C, et al. The dynamic range of circulating tumor DNA in metastatic breast cancer. Breast Cancer Res. 2014;16(4):421.
6. Rikkert LG, van der Pol E, van Leeuwen TG, Nieuwland R, Coumans FAW. Centrifugation affects the purity of liquid biopsy-based tumor biomarkers. Cytometry Part A. 2018;93(12):1207–12.
7. Taylor DD, Shah S. Methods of isolating extracellular vesicles impact down-stream analyses of their cargoes. Methods. 2015;87:3–10.
8. Canonico PG, Bird JW. Lysosomes in skeletal muscle tissue. Zonal centrifugation evidence for multiple cellular sources. J Cell Biol. 1970;45(2):321–33.
9. Lin C, Perrault SD, Kwak M, Graf F, Shih WM. Purification of DNA-origami nanostructures by rate-zonal centrifugation. Nucleic Acids Res. 2013;41(2):e40.
10. Notkins AL, Rosenthal J, Johnson B. Rate-zonal centrifugation of herpes simplex virus-antibody complexes. Virology. 1971;43(1):321–5.
11. Price CA. Centrifugation in Density Gradients. Cambridge, MA: Academic Press; 1982; 446.
12. Bagamery K, Kvell K, Barnet M, Landau R, Graham J. Are platelets activated after a rapid, one-step density gradient centrifugation? Evidence from flow cytometric analysis. Clin Lab Haematol. 2005;27(1):75–7.
13. Bagamery K, Kvell K, Landau R, Graham J. Flow cytometric analysis of CD41-labeled platelets isolated by the rapid, one-step OptiPrep method from human blood. Cytometry Part A. 2005;65(1):84–7.
14. Kattlove HE, Alexander B. The effect of cold on platelets. I. cold-induced platelet aggregation. Blood. 1971;38(1):39–48.
15. Morton BE, Hirsch CA. A high-resolution system for gradient analysis. Anal Biochem. 1970;34(2):544–59.
16. van der Pol E, van Gemert MJ, Sturk A, Nieuwland R, van Leeuwen TG. Single vs. swarm detection of microparticles and exosomes by flow cytometry. J Thromb Haemost. 2012;10(5):919–30.
17. de Rond L, Coumans FAW, Nieuwland R, van Leeuwen TG, van der Pol E. Deriving extracellular vesicle size from scatter intensities measured by flow cytometry. Curr Protoc Cytom. 2018;86(1):e43.

18. Kolesnikova IV, Potapov SV, Yurkin MA, Hoekstra AG, Maltsev VP, Semyanov KA. Determination of volume, shape and refractive index of individual blood platelets. J Quant Spectrosc Ra. 2006;102(1):37–45.
19. Chandler WL, Yeung W, Tait JF. A new microparticle size calibration standard for use in measuring smaller microparticles using a new flow cytometer. J Thromb Haemost. 2011;9(6):1216–24.
20. Simonsen JB. What are we looking at? Extracellular vesicles, lipoproteins, or both? Circ Res. 2017;121(8):920–2.
21. Boing AN, van der Pol E, Grootemaat AE, Coumans FA, Sturk A, Nieuwland R. Single-step isolation of extracellular vesicles by size-exclusion chromatography. J Extracell Vesicles. 2014;3(1):23430.
22. van Oost BA, Timmermans A, Sixma JJ. Evidence that platelet density depends on the alpha-granule content in platelets. Blood. 1984;63(2):482–5.
23. Corash L, Costa JL, Shafer B, Donlon JA, Murphy D. Heterogeneity of human whole blood platelet subpopulations. III. Density-dependent differences in subcellular constituents. Blood. 1984;64(1):185–93.
24. Boere J, van de Lest CH, Libregts SF, Arkesteijn GJ, Geerts WJ, Nolte-'t Hoen EN, et al. Synovial fluid pretreatment with hyaluronidase facilitates isolation of CD44+ extracellular vesicles. J Extracell Vesicles. 2016;5:31751.
25. Groot Kormelink T, Arkesteijn GJ, van de Lest CH, Geerts WJ, Goerdayal SS, Altelaar MA, et al. Mast cell degranulation is accompanied by the release of a selective subset of extracellular vesicles that contain mast cell-specific proteases. J Immunol. 2016;197(8):3382–92.
26. Kowal J, Arras G, Colombo M, Jouve M, Morath JP, Primdal-Bengtson B, et al. Proteomic comparison defines novel markers to characterize heterogeneous populations of extracellular vesicle subtypes. Proc Natl Acad Sci U S A. 2016;113(8):968–77.
27. Van Deun J, Mestdagh P, Sormunen R, Cocquyt V, Vermaelen K, Vandesompele J, et al. The impact of disparate isolation methods for extracellular vesicles on downstream RNA profiling. J Extracell Vesicles. 2014;3(1):24858.
28. Ghoshal K, Bhattacharyya M. Overview of platelet physiology: its hemostatic and nonhemostatic role in disease pathogenesis. Sci World J. 2014;2014:781857.

SUPPORTING INFORMATION

Additional supporting information may be found online in the Supporting Information section.

How to cite this article: Rikkert LG, Engelaer M, Hau CM, Terstappen LWMM, Nieuwland R, Coumans FAW. Rate zonal centrifugation can partially separate platelets from platelet-derived vesicles. *Res Pract Thromb Haemost*. 2020;4:1053–1059. https://doi.org/10.1002/rth2.12366